Tectonophysics 610 (2014) 138–149

Contents lists available at ScienceDirect

Tectonophysics

journal homepage: www.elsevier.com/locate/tecto

A weakening mechanism for intermediate-depth seismicity? Detailed petrographic and microtextural observations from blueschist facies pseudotachylytes, Cape Corse, Corsica

N. Deseta [a,*], T.B. Andersen [b], L.D. Ashwal [a]

[a] Department of Geosciences, University of the Witwatersrand, Private Bag 3, 2050 Johannesburg, South Africa
[b] Department of Geosciences, CEED, University of Oslo, PO Box 1047, Blindern, 0316 Oslo, Norway

ARTICLE INFO

Article history:
Received 9 July 2013
Received in revised form 16 October 2013
Accepted 3 November 2013
Available online 12 November 2013

Keywords:
Shear localisation
Intermediate-depth earthquakes
Pseudotachylyte
blueschist

ABSTRACT

Gabbro- and peridotite-hosted pseudotachylytes from the Alpine Schistes Lustres Unit in Corsica, previously determined to have formed at blueschist to lawsonite-eclogite facies conditions, have been causally linked to the generation of intermediate-depth earthquakes, which occur at depths of 50–300 km. Detailed petrographic and microtextural analyses of these pseudotachylytes suggest that their initiation may be controlled by a thermally-activated shear runaway process that is controlled by rheology rather than mineralogy. This is documented by sheared out, prolate, kinked and twinned wallrock clasts that have been peeled off and entrained into the pseudotachylyte vein as sigmoid survivor clasts. The presence of metastable high temperature crystallisation products in the pseudotachylyte, such as hoppers and dendrites of olivine, enstatite and diopside (peridotite) and Al-rich omphacite and Fe-rich anorthite in metagabbro, are suggestive of a short-lived high-temperature event resulting from thermal instability. These high temperature mineral assemblages are overprinted by ones indicating a return to ambient conditions of lower temperatures, but still high pressures: glaucophane, albite and epidote in metagabbro and clinochlore; and fine-grained granoblastic olivine, enstatite and diopside in peridotite. The observations from this detailed study of natural samples suggest that intermediate-depth seismicity may be generated by a thermal runaway process.

1. Introduction

The initiation of intermediate-depth earthquakes has long been a subject of debate. These phenomena occur at depths from 50 km to 350 km, which, due to high confining pressures, preclude traditional brittle failure (Green and Houston, 1995; Hacker, 2003; Jung et al., 2004; Ogawa, 1987). In order to address this problem researchers have put forth several hypotheses, which include dehydration embrittlement, transformational faulting and thermal runaway processes. These hypotheses can be divided into brittle — (solid-state dehydration embrittlement and transformational faulting) and crystal-plastic — (shear-heating and thermal runaway) controlled processes. These models are based on experimental, numerical and geophysical modelling, with no field observations and little work on natural samples (Green and Houston, 1995; Hacker, 2003; John et al., 2009; Kelemen and Hirth, 2007; Ogawa, 1987). In the past two decades however, several discoveries of high pressure pseudotachylytes associated with intermediate-depth earthquakes have been made (Austrheim and Boundy, 1994; Jin et al., 1998; John and Schenk, 2006; Kanamori et al., 1998), providing researchers with natural material with which to evaluate previous models. This paper presents detailed petrographic and microstructural observations of peridotite- and metagabbro-hosted pseudotachylytes associated with subduction zone seismicity, in the Cima di Gratera area of Cap Corse, Corsica. Previous work suggests that faulting and pseudotachylyte generation took place during subduction at blueschist to lawsonite-eclogite facies conditions under pressures of 1.8–2.6 GPa (Austrheim and Andersen, 2004; Andersen and Austrheim, 2006; Ravna et al., 2010; Vitale Brovarone et al., 2011). A detailed discussion on the geochemistry of these rocks and the role that water plays in earthquake generation will be addressed in a separate paper.

2. Geological setting

The study area is located on the SSW side of Cima di Gratera, Cape Corse, northern Corsica (Fig. 1). The pseudotachylytes, first described by Austrheim and Andersen (2004), occur within lenses of gabbro and mantle peridotite enclosed by serpentinite (Fig. 2). These rocks form part of the Schistes Lustres Complex (part of the Alpine age high pressure–low temperature subduction complex), and which has been interpreted as either nappes of exhumed Ligurian oceanic lithosphere, which have slivers of crystalline continental material, or hyper-stretched continental lithosphere interleaved with mantle imbricates (Agard et al., 2002; Beccaluva et al., 1977; Jolivet, 1993; Mohn et al., 2009; Vitale Brovarone et al., 2011). This rock package was thrust onto

* Corresponding author.
E-mail address: suridae@gmail.com (N. Deseta).

0040-1951/$ – see front matter © 2014 Elsevier B.V. All rights reserved.
http://dx.doi.org/10.1016/j.tecto.2013.11.007

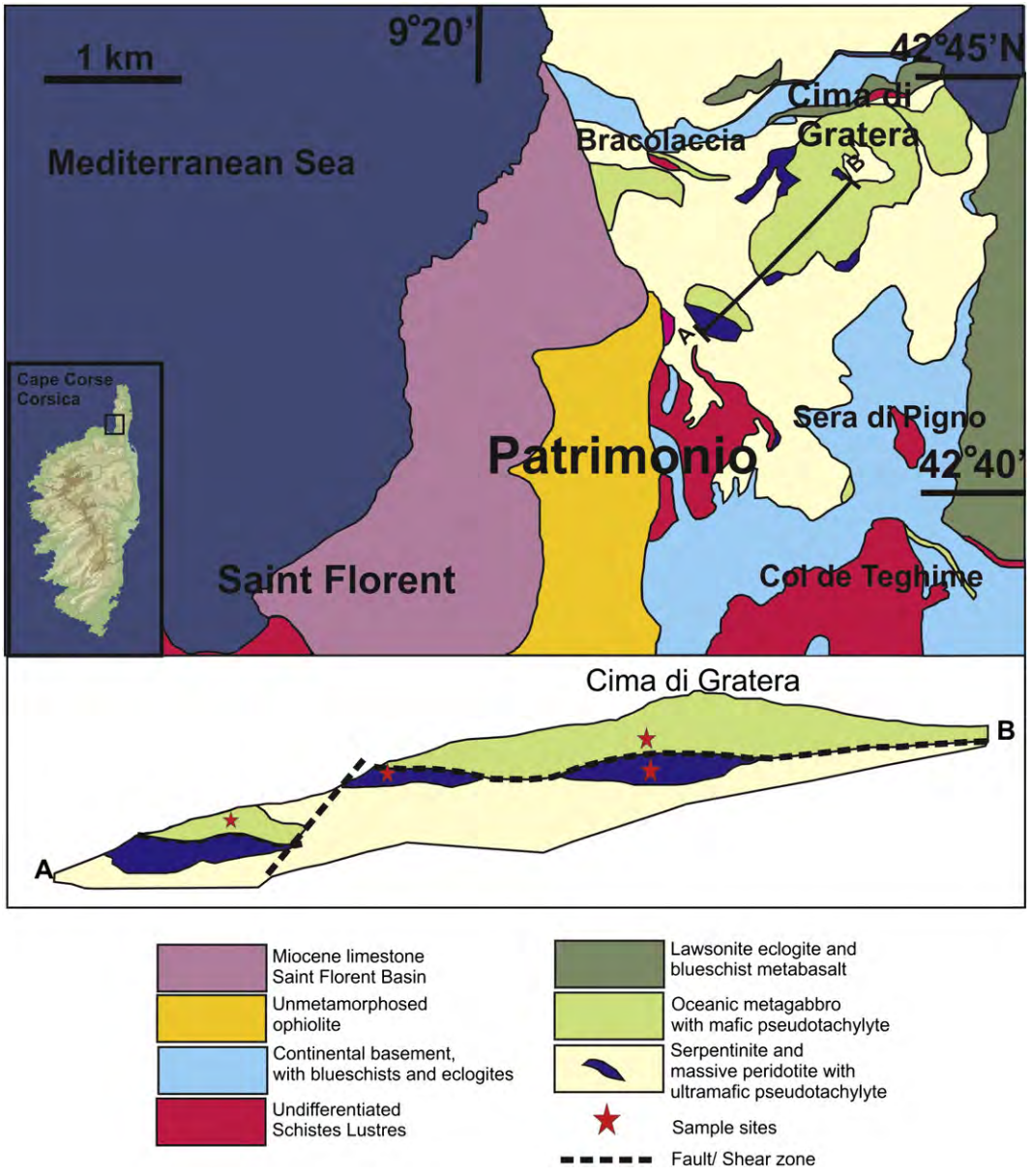

Fig. 1. Simplified geological map of the study area in Cima di Gratera. Modified after Andersen and Austrheim (2006).

the continental margin of Europe during the Late Cretaceous to Tertiary Periods (Fig. 1) (Jolivet, 1993).

The metagabbros are compositionally uniform and encompass a range of igneous textures marked by differences in grain size. Common textures are cumulate layering and the interfingering of irregularly shaped domains of fine- and coarse-grained gabbro. Conversely, the peridotites are relatively uniform in terms of composition, texture and grain size. The pseudotachylyte-bearing fault rocks have been partially metamorphosed to blueschist and greenschist facies only in patches, except within the shear zones where the metamorphic reactions are fully equilibrated. The pseudotachylytes occur within the pristine lenses of gabbro and peridotite that are relatively undeformed and least affected by the regional HP–LT metamorphism (Andersen and Austrheim, 2006).

2.1. Field observations

In outcrop the pseudotachylytes typically have a positive relief with respect to the host rocks. The pseudotachylyte veins weather to a rust-red colour but on fresh surfaces are black-grey and aphanitic (Fig. 2). Comminuted wallrock clasts and flow banding are commonly observed. In the peridotite, the pseudotachylytes occur in two sets that extend for up to 1 km: a sub-vertical set and a sub-horizontal set. Within the vein sets the pseudotachylytes form complex vein networks that over-print and re-inject one another, indicating multiple generations of pseudotachylyte (Fig. 2). In the peridotite, the pseudotachylyte veins occasionally form radial 'explosive' networks. These veins are thicker than other injection or fault veins and contain more re-injections and comminuted wallrock material (Fig. 2b). In contrast with the peridotite-hosted veins, those in the gabbro are thinner and more discrete, commonly (but not always) occurring along the boundary between the very coarse-grained (<15 mm) metagabbro and fine-grained (<2 mm) metagabbro (Fig. 2). The peridotite pseudotachylytes show cross-cutting relationships with serpentinised host rocks, which have been entrained into the veins as sigmoidal lozenges, indicating a brittle–ductile overprint relationship. In the metagabbro fault rock, the pseudotachylytic crystallisation products (glaucophane) have formed CPO (crystallographic preferred orientation) fabrics and contain boudinaged wallrock clasts, indicating a ductile overprint post-dating pseudotachylyte generation (Fig. 12) (Andersen and Austrheim, 2006). Many of the pseudotachylytes are cut by later serpentine veins and show a hydration

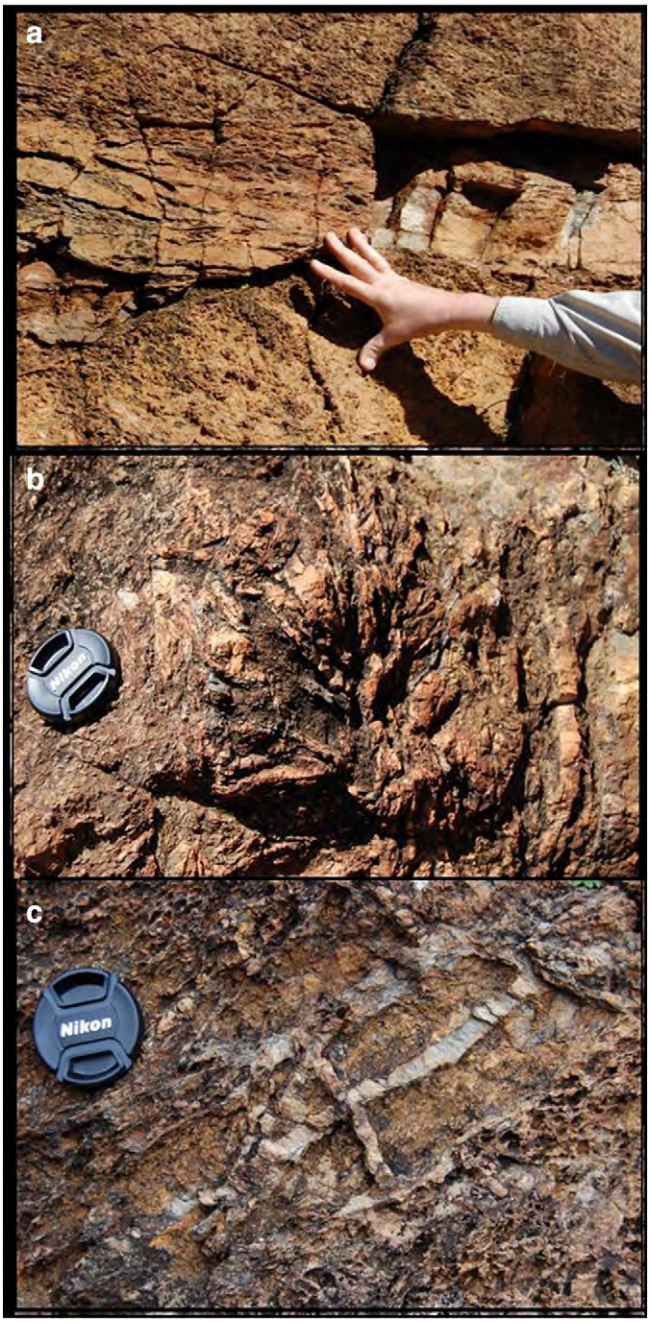

Fig. 2. Photographs of pseudotachylyte hosted by peridotite. Panel a shows one of the thickest (up to 25 cm) pseudotachylyte fault veins observed in the field. The thickness of this vein is principally due to multiple generations of pseudotachylyte that have nucleated along the same plane. (b) Explosive network veining of pseudotachylytes that radiate in all directions away from the centre of the fault plane. (c) Cross-cutting relationships of pseudotachylyte self-injecting.

overprint. Care was taken to analyse only pristine, unaltered pseudotachylytes.

3. Materials and methods

Detailed thin section petrography and back-scatter electron (BSE) imaging for mineral identification and microtextural analysis were done on both gabbro- and peridotite-hosted pseudotachylyte. Electron microprobe analyses were conducted using a Cameca SX-100 instrument at Spectrau Laboratory, University of Johannesburg, South Africa. Analyses of the bulk matrix (wide beam (10 μm) and narrow (1 μm)), wallrock, entrained minerals as well as crystallisation products (glass and crystallites) were done. The beam current was reduced to minimise sodium loss on glass, but tests on higher currents showed loss to be negligible. Analyses were run at 20 kV, 10 nA. The reference standard used was a Ni-bearing glass. Refer to Merlet (1994) for more detailed operating parameters.

4. Petrographic and microtextural observations

Detailed petrographic microtextural analyses were carried out on the pseudotachylyte and the adjacent wallrock in both the metagabbro and peridotite in order to ascertain the rheological behaviour of the rock at the time of fusion. Features of the host rocks and microtextures common to both rock types will be discussed in the first section, followed by those characteristic to only the metagabbro or the peridotite.

4.1. Metagabbro host rock

The metagabbro host rock is heterogeneous in grain size with large, irregular domains (up to approximately a metre in outcrop) of very coarse-grained (up to 15 mm) gabbro occurring in contact and interfingering with a much more fine-grained (~1 mm) gabbro. The margin between the coarse- and fine-grained domains is consistently sharp, less than 5 mm thick. Despite the large grain-size variability in the metagabbro, the constituent mineral assemblage is not significantly variable.

The primary gabbro mineralogy is largely preserved and comprises plagioclase, diopside, olivine and minor ilmenite. In thin section the gabbro adjacent to pseudotachylyte faults retains little of its original igneous texture, most of which has been transformed into an annealed granoblastic texture with poikiloblasts of olivine and diopside. Grain boundary migration and dynamic recrystallisation are common, particularly in diopside. Early greenschist facies metamorphism of the host rock has led to variable replacement and recrystallisation of diopside by actinolite, bastite and Mg-hornblende. Plagioclase alteration to sericite has also taken place, causing the grains to become cloudy and grey. Alteration of the olivine to serpentine, magnetite or iddingsite has also been observed. Post-dating the early greenschist alteration is the development of blueschist facies assemblages, which manifest in the replacement of diopside, actinolite, Mg-hornblende and plagioclase by glaucophane, barroisite, albite and epidote. Late blueschist facies metamorphism that post-dates pseudotachylyte generation at these conditions is associated with ductile deformation and pseudotachylyte recrystallisation (Fig. 12). Late retrograde metamorphism, particularly marked by serpentine veins and the presence of epidote, clinochlore and pumpellyite overprints the blueschist assemblage phase and patches of the pristine material (Fig. 13).

The early greenschist metamorphism of the host rock may be associated with seafloor hydration and/or hydration-associated fracturing in the slab bend, as well as earlier hydration associated with extensional tectonics (Mohn et al., 2009; Vitale Brovarone et al., 2011). The late greenschist metamorphic overprint has been observed in thin section and BSE images and is interpreted to be associated with hydration and faulting upon slab exhumation. This late retrograde metamorphism overprints some of the pseudotachylyte veins and is not cut by later pseudotachylyte generations (Fig. 13).

4.2. Peridotite host rock

The peridotite host rocks show gradational transitions from fine- to coarse-grained (<1 mm–7 mm) textures. The mineralogy corresponds to that of a plagioclase lherzolite with olivine > diopside > enstatite, as well as minor plagioclase and magnetite. The rocks exhibit a granoblastic texture with annealed poikiloblasts and some grain boundary migration. The diopside and enstatite commonly show exsolution lamellae of each other and twinning of the diopside and olivine has been observed.

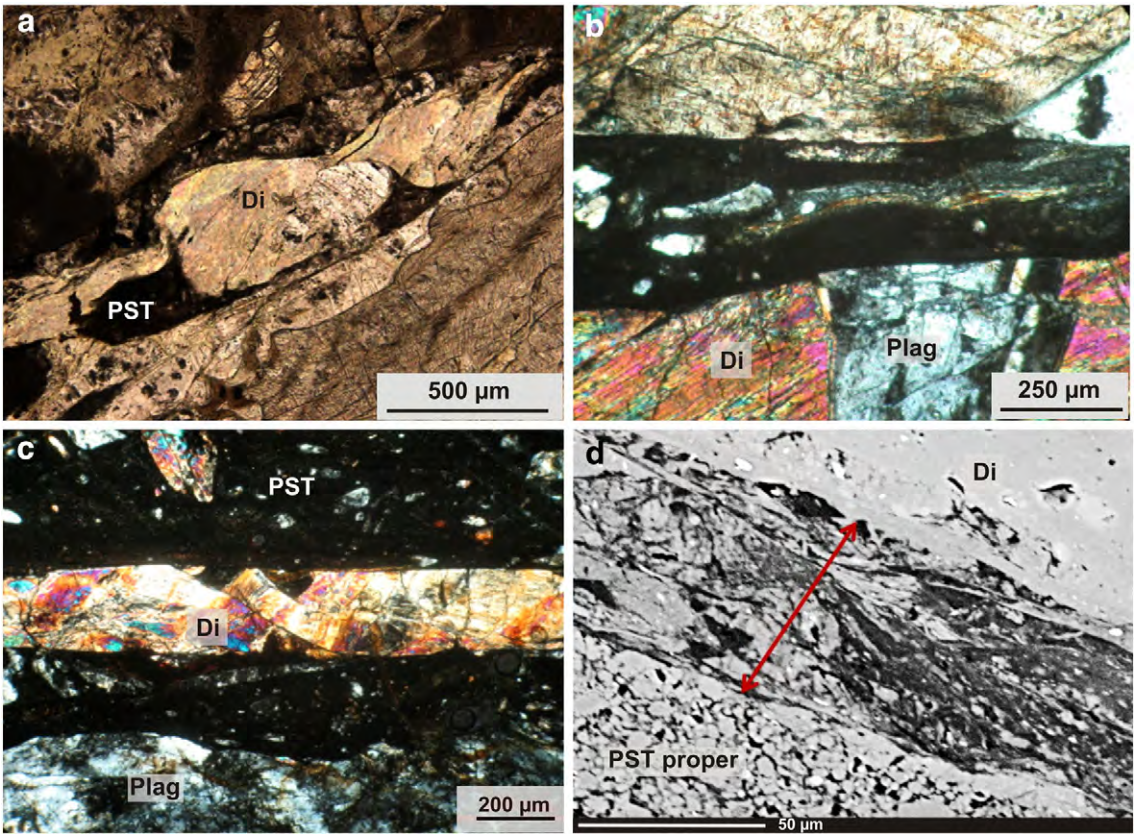

Fig. 3. Images of microstructures at fault vein boundaries in metagabbro. All these images clearly show that wallrock material at these boundaries has been subjected to crystal plastic deformation. Panel a shows a boudinaged, kink-banded diopside enclosed in a dark brown, glassy pseudotachylyte matrix. (b) Pseudotachylyte vein with entrained, boudinaged, wallrock aggregate of plagioclase and diopside. The wallrock diopside and plagioclase clearly show kinking and deformation twinning, respectively.

There is some early greenschist facies metamorphism of diopside and enstatite to fine-grained clinochlore and tremolite by dynamic recrystallisation. The clinochlore has a plumose and feathery texture. Various generations of serpentinisation (including magnetite and Cr-spinel) overprint all pre-existing features and are variably distributed throughout the rock; occasionally associated with late reactivation of pseudotachylyte veins (Fig. 12c). The peridotite shows no blueschist facies mineral assemblages; only multiple stages of early and late greenschist metamorphism are observed prior to and after the period(s) of pseudotachylyte generation. The early greenschist metamorphism has been attributed to events occurring prior to pseudotachylyte generation associated with ocean–continent hyperextension and hydrothermal alteration due to prograde subduction (Vitale Brovarone et al., 2011). The late greenschist facies metamorphism is likely associated with slab exhumation processes.

4.3. Fault vein characteristics

Fault veins form parallel to displacement surfaces in the host rock. Wallrock clasts locally underwent crystal plastic deformation in proximity to vein boundaries or melted along/with the fault plane (Fig. 3). Microscope- and BSE-based observations of the pseudotachylyte vein

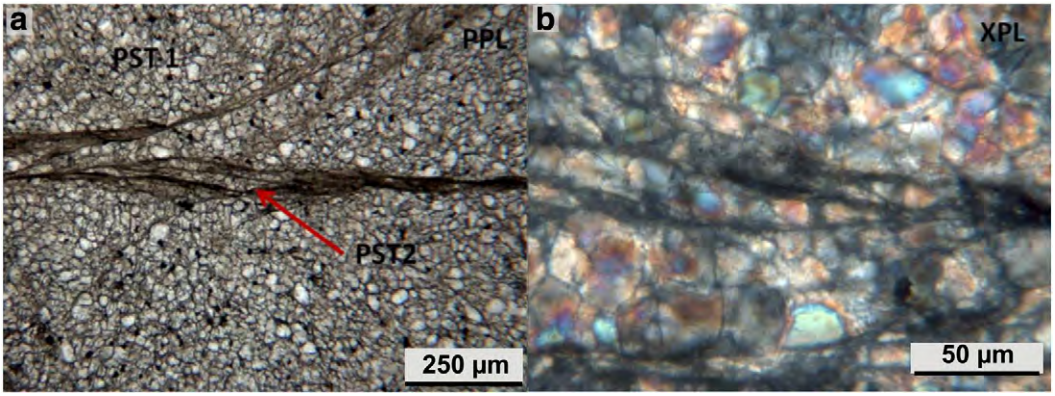

Fig. 4. Micrographs of fine-grained, recrystallized peridotite-hosted pseudotachylyte (PST 1) cut by later pseudotachylyte (PST 2). Panel b is a high magnification view with crossed nicols of where the red arrow is pointing to in panel a. In panel b the grains enclosed by the glassy black melt veins are prolate and lozenge-shaped compared to those grains not in contact with PST 2. Grain boundary migration is suggested by the grain boundary alignment of grains enclosed by fault veins. In contrast to the previous figure (Fig. 5), where coarser-grained wallrock was deformed, these photomicrographs show fine-grained recrystallised peridotite-hosted pseudotachylyte cut by a later generation of pseudotachylyte.

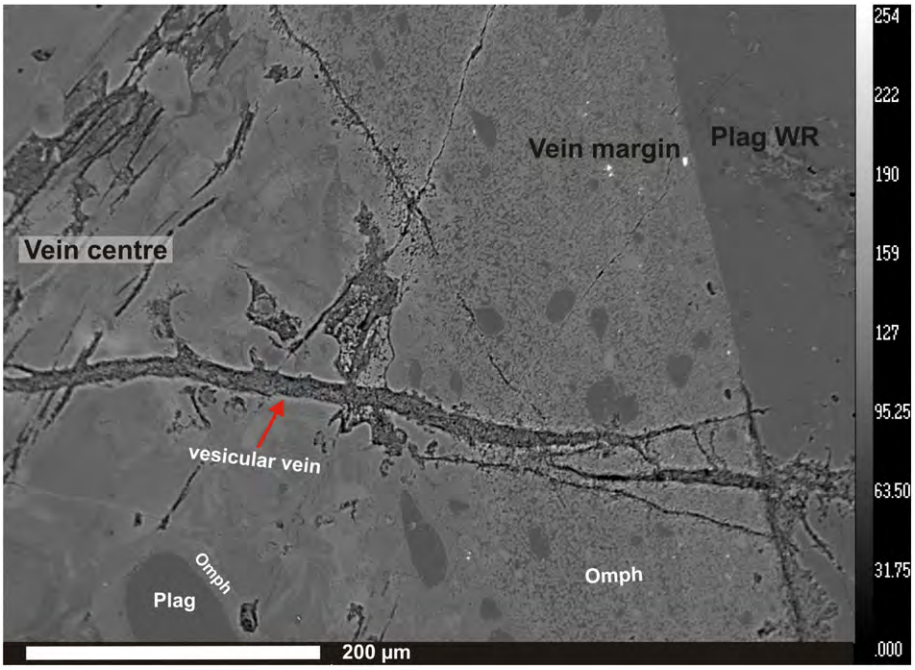

Fig. 5. BSE image of a pseudotachylyte fault vein hosted by metagabbro. The dark grey thermally rounded clasts are plagioclase upon which dendrites of omphacite have crystallised with interstitial glass. The smaller veins cross-cutting the main pseudotachylyte vein in this image, are contemporaneous with the molten pseudotachylyte, as can be seen by the lobate–cuspate boundaries enclosing the dendrites. These cross-cutting veins appear, by their low atomic numbers and low totals (on EPMA analysis) to have contained dissolved hydrous fluids that later vesiculated. Plag: plagioclase, Plag WR: Wallrock plagioclase, Omph: omphacite.

boundaries reveal a syndeformational zone in the associated wallrock that begins several grain widths from the vein 'proper'. This region is dominated by highly strained, sheared, kinked, elongate wallrock grains (Figs. 3, 6). The vein boundary is sharply cut by the pseudotachylyte and has commonly been observed to be dragged or peeled off into the vein and is surrounded by injecting melt (Fig. 3b).

Creep textures associated with the formation of the pseudotachylytes were observed in the full range of grain sizes observed in the wallrock; from 20 mm to 30 μm (Figs. 3 and 4), from shearing and kinking as seen in the coarser-grained material (Fig. 4) to what appears to be grain boundary creep in fine-grained re-crystallised pseudotachylytes that were subsequently reactivated to generate a melt (Fig. 4).

The thickness of fault veins ranges from less than 1 mm to more than 30 cm. Fault veins were typically formed by a single event. However, reactivation and multiple fusion events are exemplified by older pseudotachylyte survivor clasts entrained into younger veins (Fig. 4) and by cross-cutting relations. The lack of offset markers as well as the injection of melt into dilational fractures precludes the determination of the true dimensions of the fault zone during a single pseudotachylyte-forming event. However, due to the pristine nature of the pseudotachylyte matrices studied, we have concluded that no significant post-pseudotachylyte vein deformation occurred.

4.4. Injection vein characteristics

The injection veins are secondary pseudotachylyte veins that emanate from parent fault veins into the adjacent wallrock. Injection veins cannot in all instances be traced to their sourcing fault vein. This is due to chaotic networks of nearby multiple injection veins in proximity and arching self-injections that cross-cut one another. The veins vary widely in thickness, ranging from 200 μm, thinner than the average fault vein, to >20 cm, thicker than the average fault vein. They inject at all angles from their parent veins, from near-parallel to perpendicular. They cut between and through wallrock grains and are not associated with or dependent on precursory wallrock deformation or foliations.

4.5. Microtextures of ultracataclasite

Syndeformational ultracataclasite at the margins of coarse-grained pseudotachylyte fault veins is a common feature in both the metagabbro and peridotite host rocks. The ultracataclasite comprises a mixture of comminuted clasts, melt and plastic ribbons (Fig. 6). The size range in comminuted wallrock material is from 30 μm < 1 μm. The mineral assemblage in the ultracataclasite matches that of the adjacent wallrock. The deformation of different mineral species in the ultracataclasite appears to be determined by fracture toughness, as predicted by Spray (1992). Minerals with greater relative fracture toughness such as diopside, plagioclase, Mg-hornblende and olivine typically form the portion of comminuted grains and mineral ribbons. Softer minerals such as clinochlore, tremolite, serpentine and actinolite comprise the melt and the rest of the ribbon portion in the ultracataclasite (Fig. 6). It is possible that some of the displacement in the fault veins is accommodated by preferential crystal plastic deformation and fusion within the ultracataclasite, explaining the lack of kinematic markers between the fault vein pseudotachylyte and wallrock (Kim et al., 2010; Sibson, 1980; Spray, 1992). The microtextures of this unusual crystal-plastic ultracataclasite may hold information regarding the earliest stages of pseudotachylyte generation. It is important to take note that no ultracataclasite appears to form in pseudotachylyte fault veins hosted by equigranular, fine-grained rock (~20 μm) in both the peridotite and metagabbro.

4.6. Microtextures of the pseudotachylyte matrix

The matrices of the metagabbro and peridotite pseudotachylytes are typically dominated by crystallisation products of the melt, with interstitial crypto-crystalline material or glass and entrained wallrock clasts that vary greatly in size and can constitute up to 20% of the vein, but are normally much less. The presence of interstitial glass was confirmed with XRD synchrotron analysis (Fig. 8). The veins are commonly marked by streaks or colour bands that indicate compositional variation, predominantly due to clusters of spinel, and inefficient mixing of the melt

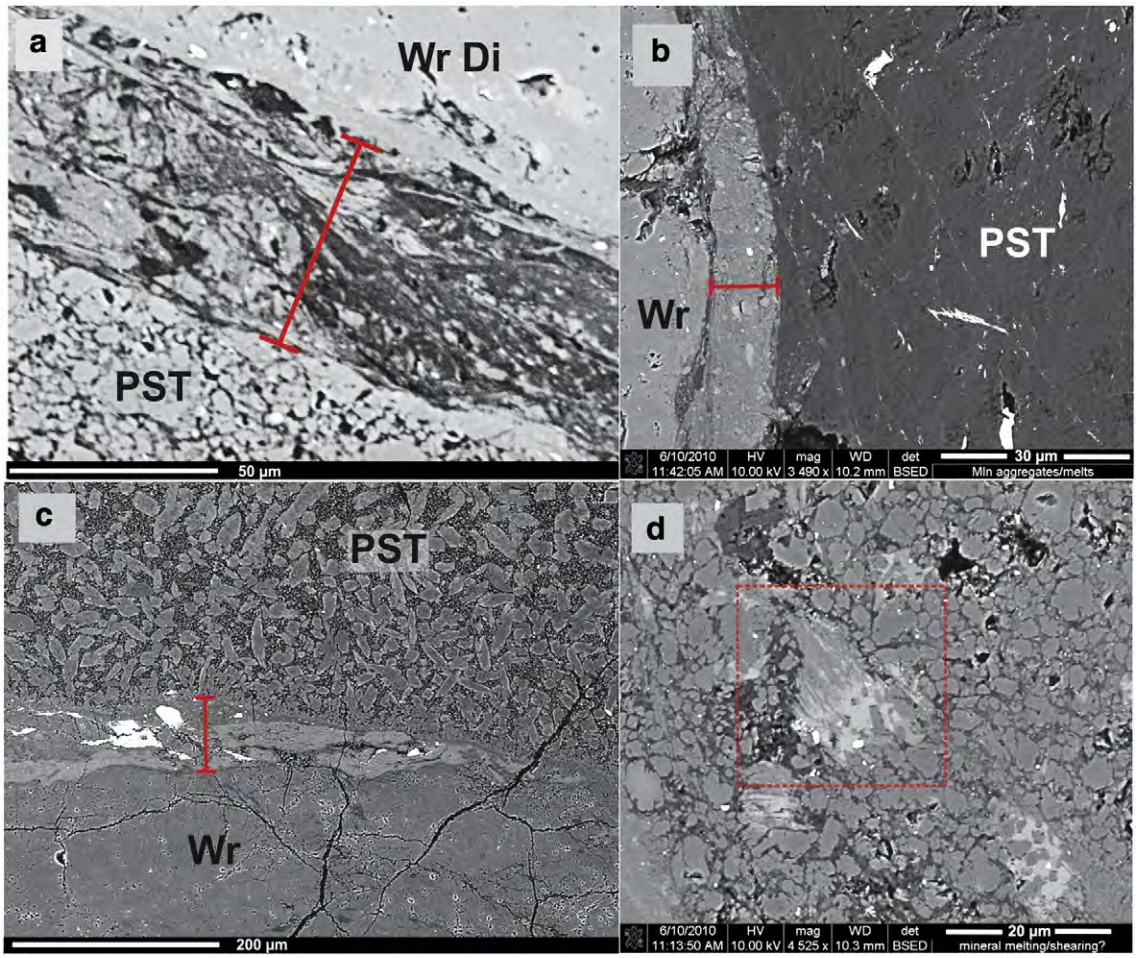

Fig. 6. BSE images a–c of ultracataclasites at fault vein boundaries in peridotite. A range of brittle–ductile textures are present in the ultracataclasite, the width of which is shown by the capped red line. (a) Close-up of the ultracataclasite; the black areas are a hydrous Al-rich melt, the dark grey areas are a sheared out pseudotachylyte matrix, and the lighter grey is a combination of sheared out survivor clasts of wallrock diopside and pseudotachylyte matrix. Image d shows a pseudotachylyte matrix crystallising olivine (grey) and diopside (light grey) in a hydrous matrix (dark grey). The red box encloses an olivine–diopside crystal complex being sheared out prior to total solidification indicating continued displacement along fault veins post melt production and failure. Panel c shows a similar feature; brittle-looking ultracataclasites with a matrix hosting ribbons of stretched out diopside microlites (in white). Wr: Wallrock, Wr Di: Wallrock diopside grain.

(Fig. 7). The crystallisation products have various habits: hopper crystals, simple acicular laths, and feathery plumes, which nucleate on clastic material in the vein forming dendrites or along vein boundaries. A principal control on microlite size is the presence or absence of a nucleation surface and the size of this surface. When the nucleating surface is particularly small it generally forms the core of a larger than average complex dendrite composed of several mineral species. Space may also exert a control on crystallisation; areas that appear to be

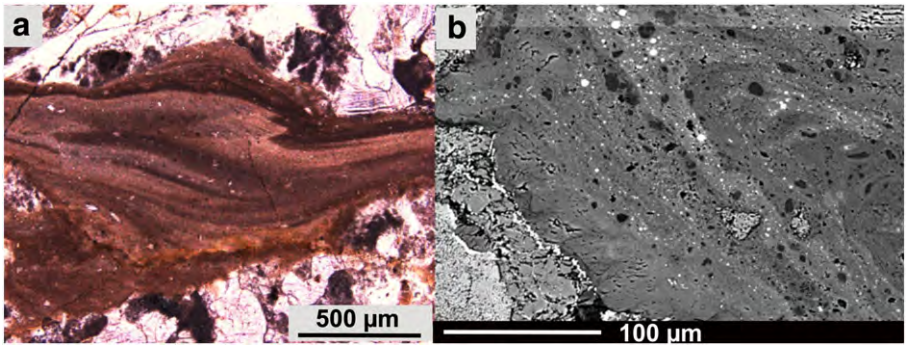

Fig. 7. Micrograph (a) and BSE image (b) of pseudotachylyte matrix in a metagabbro. Colour bands in these veins are evident in both images and are attributed to zones where individual minerals or aggregates have fused and become decrepitated and sheared out. Clusters of microlites and glassy material are also observed to form bands. However, the crystallisation products of the melt are strongly controlled by its composition, and hence the pre-existing minerals that fused will be the dominant control over the formation of these colour bands. Minimal physical sorting or fractionation has been observed in these veins, so this is not considered to be a significant factor.

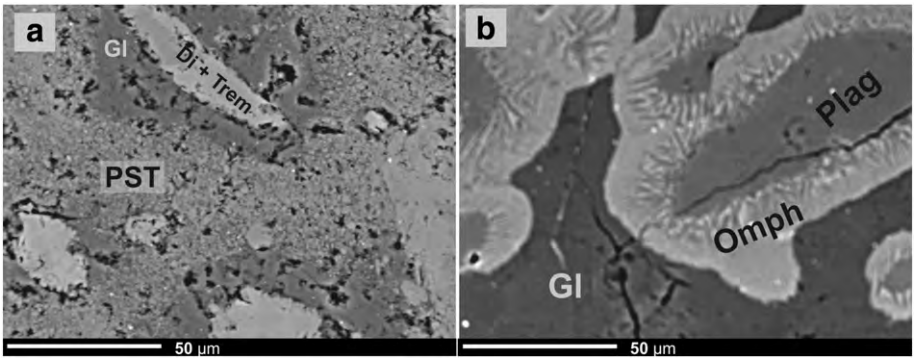

Fig. 8. BSE images of individually fusing clasts enclosed in a pseudotachylyte matrix. (a) The matrix is dominated by microlites and minute relict clasts. However, at the boundary of melting clasts there is a zone of Al-rich, hydrous glass (Gl). Conversely, in panel b the matrix is glass dominated (anhydrous) and the fusing grains are bounded by a crystallisation front of Al-rich omphacite (Omph) nucleating on plagioclase (Plag) derived from wallrock. Di + Trem: aggregate clast of wallrock diopside and tremolite.

absent of any nucleating surface are typically host to some of the largest crystals.

4.7. Microtextures of survivor clasts

Survivor clasts comprise wallrock material that has been dragged into the pseudotachylyte during its formation. These can be monomineralic or composed of aggregates of minerals. They are typically angular or tabular in shape, with thermally rounded margins. The larger tabular forms are aggregates from the deformed wallrock that have been scoured away from the vein boundary by injecting melt (Fig. 3). The composition of the clasts is the same as that of the adjacent wallrock mineralogy, but not in the same proportions. Hydrous minerals such as Mg-hornblende, clinochlore and serpentine occur only in rare aggregates with anhydrous minerals and are thus inferred to have melted preferentially. Monomineralic olivine, diopside, magnetite, ilmenite and plagioclase have all been observed in the matrix of both types of host rock. Diopside and plagioclase are the most common clasts derived from the metagabbro host rock, whilst olivine and diopside are those abundantly found in the peridotite. Survivor clasts commonly exhibit undulose extinction and kink-banding similar to that observed just beyond fault vein boundaries in the wallrock, suggesting that they may be derived from the wallrock and underwent similar crystal plastic deformation. Sieve textures in sheared out wallrock and partially resorbed survivor clasts of older pseudotachylyte have also been observed (Fig. 9).

Further detailed petrographic data have been divided according to the metagabbro and peridotite host rocks. Within those groups the most pristine samples were selected for microtextural and geochemical analysis. The pseudotachylytes are highly heterogeneous in composition down to the micron scale, so this separation is the best way to gain information from these veins and interpret their mechanism of formation meaningfully.

4.7.1. Metagabbro: pseudotachylyte

Compositionally the pseudotachylytes hosted by metagabbro are highly heterogeneous, strongly reflecting local mineral compositions of the adjacent wallrock and survivor clasts. However, despite the compositional variability of the melt, the mineralogy of the crystallisation products in the pseudotachylytes is simple albeit showing great chemical variability. The pseudotachylyte matrix is defined as a combination of glass, crystallisation products and comminuted material that are too small to be resolved by electron microprobe analysis (EPMA) beam (<1 μm). The crystallisation products are divided into two groups: a high temperature quench assemblage with pockets of interstitial glass, and a lower temperature assemblage in which devitrification of the glass and recrystallisation of the pseudotachylyte matrix have taken place.

4.7.1.1. Microlite assemblage in the metagabbro pseudotachylytes. This microlite assemblage is dominated by omphacite and plagioclase, with minor ilmenite (Fig. 10). This is the first reported evidence of natural crystallisation of omphacite directly from a melt. Omphacite has been reclassified from fassaite, as it was termed by Andersen and Austrheim (2006). The composition of the minerals is highly variable and is strongly controlled by melt composition in the matrix or by fusing

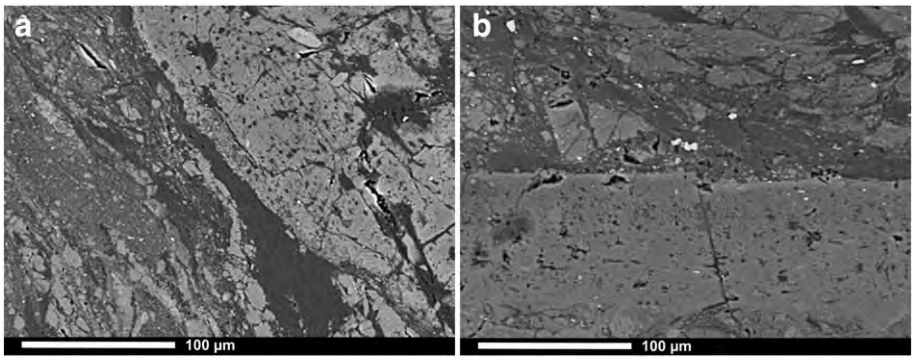

Fig. 9. BSE images of sieve textures in a peridotite-hosted pseudotachylyte matrix. Both panels a and b show at least two generations of pseudotachylyte. The sieve textured material in both images is the oldest generation that has been deformed and partially digested by a younger pseudotachylyte generation into which sheared out clasts of the older pseudotachylyte have been entrained. The oldest generation of pseudotachylyte contains inclusions of relative low atomic number (and low totals when analysed with EPMA; ~86%), suggesting that these are quenched melt inclusions with fluids dissolved in them to varying degrees. Preliminary Raman spectroscopy shows these vesicles to contain glassy material and empty cavities, presumably once filled with fluid.

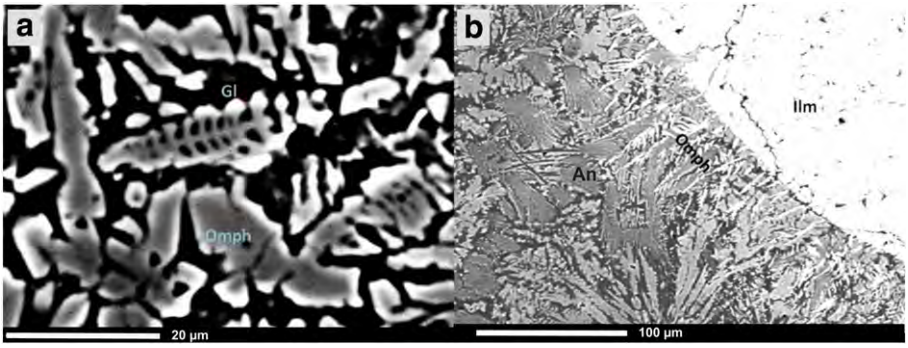

Fig. 10. Omphacite is the principal high temperature mineral crystallising from gabbroic pseudotachylyte, with anorthite and ilmenite to lesser degrees. Panel a shows delicate, zoned hopper crystals of omphacite enclosed by glass; this crystal habit is an indicator of rapid, high temperature quenching. Panel b shows omphacite in white and light grey with feathered and dendritic textures. The dark grey dendrites are anorthite. The variation in the composition of omphacite is controlled by the mineral that it nucleates on, as shown by the change in greyscale; its local melt composition and zoning in the crystals. Omph: omphacite, Ilm: Ilmenite.

clasts on which the microlites have nucleated. The omphacite is characterised by significant Al-enrichment relative to typical omphacite, which could be due to the high temperature and pressure of crystallisation (average Al_2O_3: 17.3 wt.%). The plagioclase is characterised by high FeO_{total} and MgO contents (average FeO_{total} = 1.3 wt.%, MgO = 1.1 wt.%), possibly due to the rapidity or high temperature of crystallisation, or inclusions of unresolvable omphacite or ilmenite. These microlites take the form of laths, dendrites and skeletal hoppers crystallising freely in the pseudotachylyte matrix or nucleating on vein boundaries or on survivor clasts. The omphacite is clearly zoned with Mg-rich cores and Fe-rich rims (Fig. 10).

4.7.1.2. Metagabbro: devitrification and recrystallisation of pseudotachylytes. Devitrification of glass and recrystallisation of the higher temperature minerals that quenched directly from the pseudotachylyte melt produce its own assemblage of blueschist facies minerals: glaucophane, Fe-rich albite, epidote and minor sphene (Fig. 11a, b). The crystals in this assemblage are commonly coarser than those in the higher temperature assemblage (up to 2 mm). They are also more irregular and blocky in form, no longer exhibiting the dendritic habits of the replaced minerals. They occasionally show a deformation fabric expressed as folds and boudins of pseudotachylyte at the thin section scale, indicating a ductile blueschist facies overprint (Fig. 12a).

4.7.2. Peridotite: pseudotachylyte

At the millimetre to micron scale the peridotite pseudotachylytes show great variability in composition and abundance of bulk matrix, glass and crystallisation products. Despite this variability, the microlites consistently comprise diopside, olivine and enstatite. As with the metagabbro, the peridotite fusion products can be divided into a high temperature quench assemblage and a lower temperature devitrification assemblage.

4.7.2.1. Microlite assemblage in peridotite-hosted pseudotachylytes. Olivine, diopside and enstatite occur as clusters of monomineralic blocky microlites (particularly olivine) or as dendritic complexes. Also common are larger, polymineralic laths and dendrites (Fig. 11). The interstitial material of the bulk matrix ranges is a variable mixture of olivine and enstatite and has an H_2O content ranging from 0 to 14.2 wt.% H_2O.

4.7.2.2. Peridotite: devitrification and recrystallisation of pseudotachylytes. Devitrification of glass and recrystallisation of the higher temperature minerals that quenched directly from the pseudotachylyte melt produce distinct assemblages. Typically the devitrified melt is characterised by the formation of microfibrous clinochlore, serpentine and tremolite (Fig. 9). In contrast, pseudotachylyte that has completely recrystallised comprises fine-grained (<50 μm) granoblastic diopside, olivine and enstatite (Fig. 4).

5. Discussion

The microtextures analysed in this study are spatially and temporally associated with pseudotachylyte generation. The observed crystal–plastic phenomena that are considered to be causally linked to fusion and seismic failure include: dislocation creep/glide, deformation twinning, kinking, bending and ultracataclasite/melt formation (Figs. 6 and 13). The ultracataclasite observed in these rocks is unusual in that it contains angular comminuted wallrock minerals as well as ribbons and strings of minerals exhibiting syndeformational ductile features (Fig. 6). The interstitial areas of the ultracataclasite contain glassy pockets of preferentially melted hydrous minerals, e.g. tremolite and clinochlore. Together, these textures suggest that the wallrock minerals may have undergone power law creep-dominated deformation that reached seismic strain rates, to induce the heating and fusion of the wallrock that is characterised by the presence of pseudotachylyte in these rocks (John et al., 2009; Kameyama et al., 1999).

The quench products of the pseudotachylytes indicate initially very high temperatures (~1600 °C), followed by a return to blueschist to lawsonite-eclogite conditions (~430 °C–550 °C, 1.8–2.6 GPa) (Andersen and Austrheim, 2006; Ravna et al., 2010). When the pseudotachylytes devitrify or recrystallise, the resulting mineral assemblages (glaucophane, albite and epidote in the metagabbro and diopside, olivine, enstatite and clinochlore in the peridotite) indicate a high pressure, low temperature environment (Ravna et al., 2010).

5.1. Precursors to pseudotachylyte formation

To date, several mechanisms have been put forward to explain the initiation of intermediate-depth seismicity. They all share the commonality of being fundamentally dependent on precursory conditions (Green and Houston, 1995; John et al., 2009; Kelemen and Hirth, 2007). Therefore, we need to investigate in detail the evidence of any preserved pre-existing elements that may elucidate the sequence of events that culminate in the production of these high pressure pseudotachylytes. A close spatial relationship between pseudotachylyte formation and fabric development is observed in the host rocks. This is not a unique occurrence and has been noted by previous workers in other pseudotachylyte studies (Bestmann et al., 2011; Hobbs et al., 1986; Jin et al., 1998; Kim et al., 2010; Lin, 1994; Lund and Austrheim, 2003). Hobbs et al. (1986) were amongst the first to propose the possibility that in high pressure cases, pseudotachylyte and mylonite formation may be inter-related processes; suggesting that at the highest deformation rates pseudotachylyte would form, followed by cataclasis

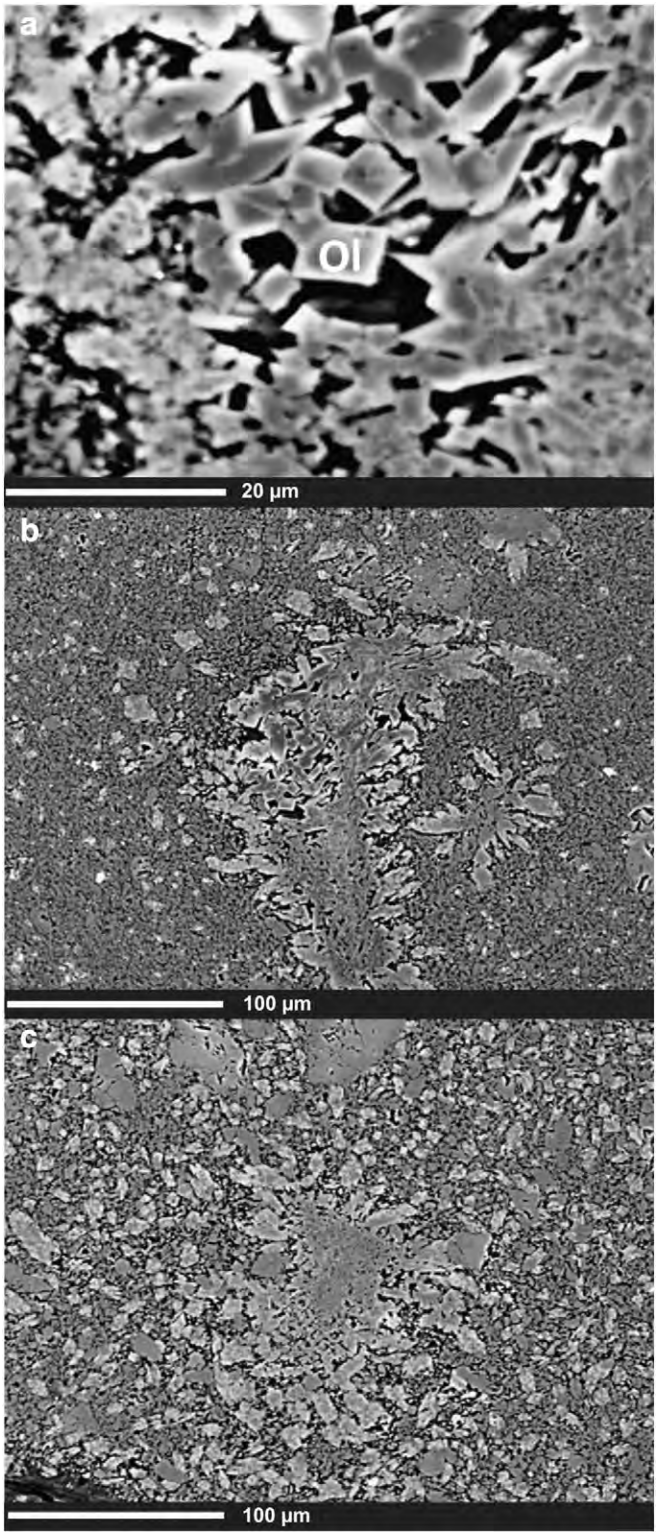

Fig. 11. BSE images showing the three principal types of crystallisation styles in peridotite hosted pseudotachylyte. Panel a shows blocky microlites of olivine surrounded by glass (black in images). The olivine crystals show strong Mg–Fe zoning from core to rim. Panel b shows pure olivine dendrites clustered in an aggregate with interstitial glass in a matrix of blocky olivine crystals and complex laths of diopside (light grey) and olivine (darker grey). (c) This image shows an aggregate of crystallised material in the centre. Close inspection shows that the aggregate is composed of three minerals; enstatite (darkest grey), olivine (mid-grey) and diopside (light grey). The aggregate is dominated by these complex, tri-mineralic dendrites. The black interstitial matrix in all three images was analysed to be a variably Al-, H_2O-enriched glassy material.

and then fabric development, potentially culminating in mylonite at the lowest deformation rates.

Incipient fabric development prior to and after pseudotachylyte formation has been observed (Figs. 6d, 12a, 14). Detailed EBSD analysis of a peridotite fault section from the same field area shows that the wallrock minerals are exposed to increasing strain towards pseudotachylyte fault veins. The wallrock has undergone recrystallisation to form an incipient lattice preferred orientation (LPO) prior to and/or during fault vein development (Silkoset, 2013). Crystal plastic deformation such as folding, boudinaging, annealing and foliation development occurring after fault vein formation has been observed within veins and the associated wallrock (Figs. 6d, 12, 14). The time lapse between pseudotachylyte generation and fabric development (before and after) is unknown. However, the simplest explanation of the observations involves: recrystallisation in the wallrock with increasing strain towards vein boundaries as well as rotation of elongate wallrock clasts into parallelism with developing fault vein boundaries. Continued shearing (Fig. 6) occurs after displacement and fusion have taken place, at which point the fault zone had cooled enough to crystallise glaucophane (in the metagabbro) and clinochlore (in the peridotite). We suggest the following sequence of events to explain our observations:

The majority of wallrock material for both metagabbro and peridotite is coarse-grained and partially deformed due to previous events. As a result the wallrock grains will likely contain numerous crystallographic imperfections that can be exploited when in the right orientation in the stress field to form the loci of fault nucleation and initial fusion due to low temperature creep, followed by power law creep.

1. The fault wallrocks developed a damage zone with synchronous recrystallisation and an increasing strain-gradient towards the future fault plane as also observed by Silkoset (2013).
2. Anisotropic wallrock fragments have rotated so that long axes become parallel with the developing slip surface.
3. Deformed wall-rock fragments become entrained, as survivor clasts in the pseudotachylyte melt and their deformation is associated with the shearing event that produced the melt. Some undergo near complete to complete fusion.
4. In some veins, shearing and displacement continued after fusion, locally attested to by deformed and recrystallised pseudotachylyte.
5. Pseudotachylyte and fault damage zones cooled down sufficiently to devitrify or recrystallise to glaucophane (in metagabbro) and clinochlore (in peridotite).

It is possible that at lower deformation rates foliations may develop in the pseudotachylyte and wallrock between major faulting events.

Based on the observations and sequence of events presented above, we suggest the following model for pseudotachylyte generation:

The metagabbro and peridotite were mostly coarse-grained rocks, but both host rocks had structural and mineralogical heterogeneities inherited from earlier events. During subduction-related deformation, pre-existing zones with numerous crystallographic imperfections at favourable orientation relative to the new stress field become the loci of enhanced deformation (Jessell and Lister, 1991; Kameyama et al., 1999; Sibson, 1980). Low temperature and subsequent power law creep, induced by seismic strain rates eventually gave rise to fusion. It is possible that several loci in the same orientation underwent contemporaneous strain-induced fusion. These individual melt spots may in turn have linked up to form primitive fault planes. Stick-slip action along such plane will be preferentially activated for further slip and facilitate comminution and fusion. As the stress is released by comminution, displacement and fusion, the temperature of the fault and damage zone will remain elevated until the stress has dropped below the strength of the transient melted material of the fault. Thereafter, heat is dissipated by diffusion beyond the cooling vein and damage zone to facilitate crystallisation of the wallrocks. The delicate preservation of quench textures in pseudotachylytes suggests neglible post-quenching

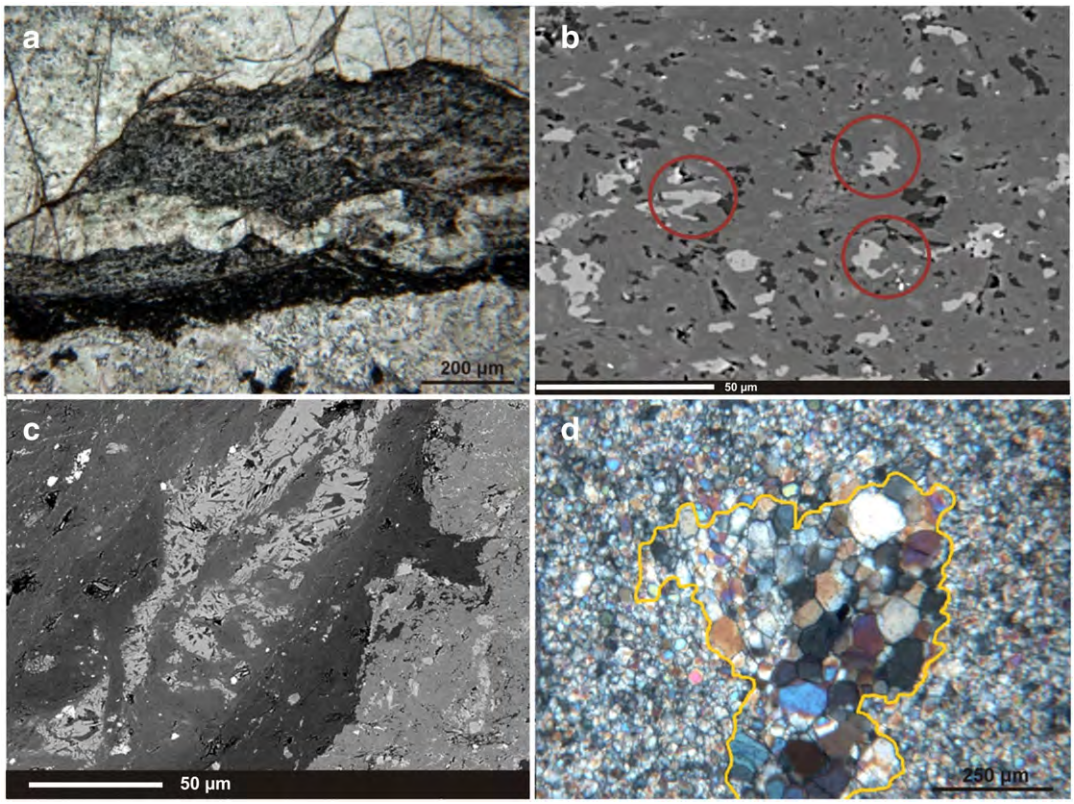

Fig. 12. Micrographs and BSE images showing the various recrystallisation textures in pseudotachylytes from both host rocks. Panels a and b metagabbro pseudotachylyte (a) from the same thin section sample as panel b, only at a lower magnification. (a) Folding of the recrystallised pseudotachylyte. The microlites in panel b are blocky, no longer the dendritic forms shown in previous examples. EPMA analyses show the mineral assemblage to be glaucophane, sphene (light grey crystals), albite (dark grey crystals) and epidote (darkest grey). The crystals are subhedral and deformed and aligned in a subtle fabric due to folding, as shown in panel a. Images c and d: peridotite–pseudotachylyte. (c) A devitrified pseudotachylyte matrix that has an ultrafine (<1 µm) of clinochlore composition. The matrix is not recrystallised as pristine quenched dendrites of diopside are observed (light grey dendrites (c) and stretched out, deformed clasts are evident along with zoning/colour banding in the vein that are preserved. Panel d shows a recrystallised matrix; the yellow line indicates the form of a recrystallised wallrock aggregate that was entrained into the pseudotachylyte. The surrounding fine-grained material comprises olivine and enstatite clasts which have replaced earlier dendrites and upon stage rotation under the microscope, shadows of now replaced dendrites can be observed. The clasts in this photomicrographs are annealed, forming a granoblastic texture and show no evidence of deformation. It is important to note that peridotite pseudotachylyte recrystallises to a harzburgitic composition.

deformation in most of the pseudotachylyte veins except in those areas where later regional deformation and metamorphism are penetrative.

5.1. Possible influence of grain size on pseudotachylyte formation

The grain size of both the metagabbro and the peridotite ranges from approximately 20 µm–260 µm. The principal deformation mechanism of the wallrock material and entrained survivor clasts that have been sheared and kinked but show no evidence of crystallographic recovery prior to pseudotachylytic fusion is interpreted to be dislocation creep/glide. EBSD analysis in a recent study indicates that the wallrock encountered rapidly increasing strain towards the pseudotachylyte boundaries, with weakly developed LPOs (Silkoset, 2013). The incipient LPO development could be due to localised stresses in the rock being accommodated by high dislocation densities in different grains (Branlund et al., 2000; Kameyama et al., 1999; Newman et al., 1999). EBSD analysis by Silkoset (2013) and intracrystalline microtextural observations (Figs. 3) in this study suggest dislocation creep as a possible dominant deformation mechanism associated with pseudotachylyte formation. If this is the case then there would be little grain size reduction through dynamic recrystallisation associated with the instability as diffusion creep would be a secondary deformation mechanism (Kameyama et al., 1999; Kelemen and Hirth, 2007). In finer-grained material (grain-size approximately 20 µm) strain has been accommodated by grain boundary sliding as opposed to intra-grain deformation; grain boundaries associated with the pseudotachylyte are aligned and grains appear squamous in shape as opposed to equant (Fig. 4).

It appears that higher volumes of melt are formed in the coarser-grained host rock. Of course, the current fault and injection vein thicknesses are not expected to be an exact indication of melt volume. However, taking vein dilation, draining and deformation into account the melt volume produced by coarse-grained rock relative to fine-grained rock is orders of magnitude greater; refer to Fig. 2a vs Fig. 4 where an outcrop scale image of an average fault vein is compared to the largest fault vein observed in the finest grained host rock, seen in thin section as it is so small. This may correspond with power law creep as a principal deformation mechanism as coarser-grained material would be easier to deform than finer-grained material. Coarser grains can accumulate more dislocations and higher dislocation densities in local areas of slip than can finer grains suggesting a greater potential for localised heating (Kameyama et al., 1999). Images of pseudotachylyte in the finer-grained host rock (Fig. 4) suggest that grain boundary sliding occurs preferentially over intra-grain deformation to resolve the applied stress.

Furthermore, our geochemical results show that grain size influences melt composition such that the bulk composition of a pseudotachylyte derived from a fine-grained host rock will better approximate fusion akin to that of an equilibrium melt (this is due to melt formation occurring primarily along grain boundaries), whereas in pseudotachylyte derived from a coarser-grained host, the bulk melt composition tends to reflect wholesale fusion of individual minerals such as olivine or diopside.

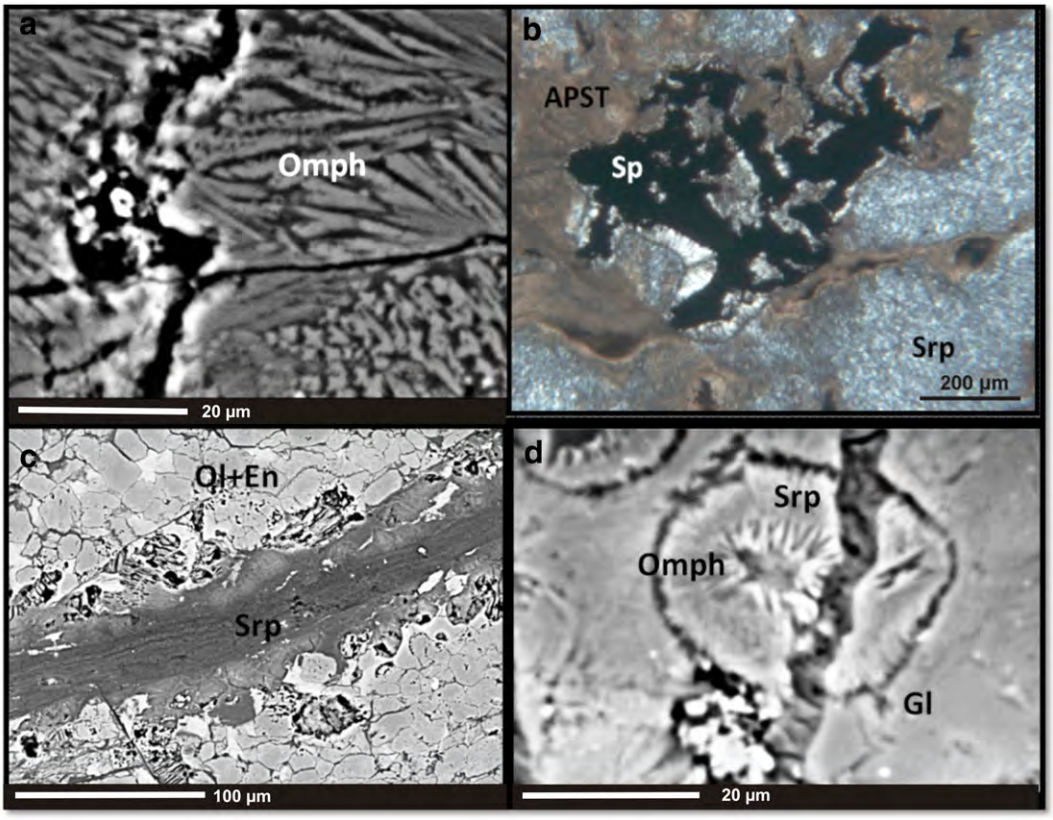

Fig. 13. BSE images and a photomicrograph (b) of hydrated/altered pseudotachylyte. In all images serpentine and associated spinel is the principal late alteration mineral (as is the case in both host rocks), but late epidote and actinolite are also present in the metagabbro. These images show how serpentinisation destroys the delicate textures associated with the pseudotachylyte forming event (dendrites and vein boundaries) and bleaches the pseudotachylyte, removing magnesium. (a) A black vein crosscuts a pristine pseudotachylyte matrix of omphacite in a metagabbro. The boundaries of the vein can be seen on BSE to have bleached the matrix enriching it in Fe. (b) Serpentinised peridotite pseudotachylyte where all microscopic crystallisation textures have been obliterated. (c) A late serpentine vein cuts through a recrystallised peridotite pseudotachylyte. Microfibres of serpentine can be seen eroding the fine-grained granoblastic texture. (d) Serpentine vein crosscutting spherulitic omphacite in an otherwise glassy pseudotachylyte matrix. Ol: olivine, En: enstatite, Srp: serpentine, Omph: omphacite, Gl: glass, Sp: spinel APST: altered pseudotachylyte.

Grain size reduction adjacent to vein boundaries was observed from the outcrop scale to the micron scale. Microtextural relationships suggest that this change in grain size is a feature contemporaneous with pseudotachylyte generation and is due to intense shearing along the fault surface, whereby the heat released by shearing facilitates recrystallisation and the shearing itself induces the reorientation of wallrock clasts and/or their comminution. This is in contrast with the results of Kelemen and Hirth (2007) and John et al. (2009) where a pre-existing fine-grained zone in the host rock was proposed in order to provide a nucleation site for shear instabilities to take place.

5.2. Present model compared to previous mechanisms

The Corsican pseudotachylytes contain up to 15 wt.% H_2O. This coupled with the large melt volumes produced by these events, apparently precludes dehydration embrittlement as a mechanism for the observed paleofaults. There is no evidence that free water or other fluids were available before faulting. Previous work by Green (1973), Jung et al. (2004) and Kirby et al. (1991), indicates that dehydration embrittlement is related to a solid-state monomineralic reaction. Its occurrence in polymineralic materials such as those studied here has to our knowledge not been tested experimentally. Instead we suggest that the high

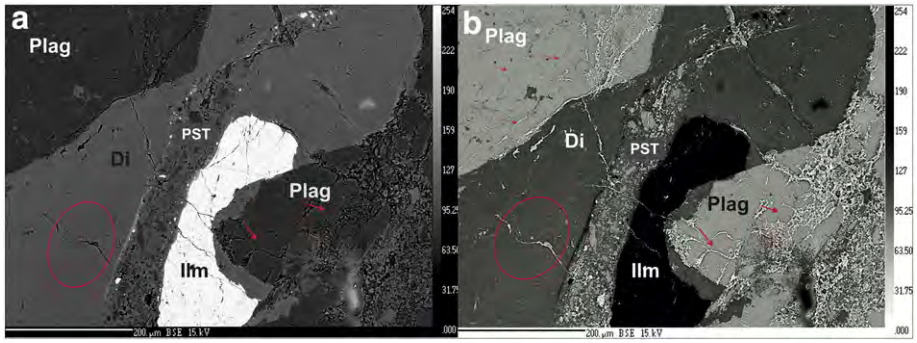

Fig. 14. BSE image of metagabbro with several generations of pseudotachylyte. The image on the left is the original BSE image and the image on the right has been inverted to highlight some features. The red circle highlights kinkbanding in wallrock diopside (Di). A minute fault vein has formed within a kink plane. The arrows indicate preferential fusion in the plagioclase (Plag) along certain planes. The white clast in the centre is ilmenite (Ilm).

temperature deformation related to local shear-heating was more significant for failure than a solid-state dehydration reaction weakening. Previously published shear heating models (John et al., 2009; Kelemen and Hirth, 2007) are not perfect fits either. Both these models prescribe precursory mylonites or fine-grained zones that act as strain concentrators in order to initiate self-localisation. Our observations from the rocks in Corsica however, indicate that, despite various differences in the host rocks, seismic faulting and fusion took place regardless of grain size, rock fabric or composition. The only discernible restriction on mineralogy is fracture toughness; minerals must have a shear yield strength great enough to allow for a sufficiently large stress build-up (Spray, 1992), which explains why no pseudotachylytes occur in the serpentinites surrounding the peridotite and metagabbro blocks. A non-quantified and speculative option may be that the rheological behaviour of rocks traditionally predicted at high pressure may not be simply constrained by visco-elasticity or Von Mises Criterion as suggested by (Mancktelow, 2006).

6. Conclusions

Both shear instabilities and dehydration reactions are thermally activated processes. However, the activation of thermal instability is derived from local rheological heterogeneities that provide a viscosity contrast in the host rock material at sufficiently high stresses that it behaves as a non-linear viscoelastic material (Braeck and Podladchikov, 2007; John et al., 2009; Kameyama et al., 1999; Ogawa, 1987). Conversely, dehydration embrittlement is induced by warming of the previously hydrated slab making it dependent on the presence of pre-existing hydrous mineralogy and an efficiently warmed slab. In addition, there is no evidence in the petrographic data to support the hypothesis of a dehydrated precursor to pseudotachylyte nucleation. This is not to say that dehydration embrittlement does not occur; it may well occur in the serpentinite enclosing the blocks of peridotite and metagabbro. The results from this study suggest that these pseudotachylytes produced at high pressure and seismic strain rates, in different host rocks, with different degrees of hydration, may have been generated by a high temperature crystal-plastic shear process. Detailed petrographic analysis suggests that low temperature and power law creep may play dominant roles in producing thermal instabilities and high pressure pseudotachylytes. Deformation of wallrock grains at the boundary of fault veins results in the formation of subtle LPOs in olivine grains and grain size reduction due to comminution (Silkoset, 2013). These features form at the onset of and during pseudotachylyte generation, not before, and they are not the precursory elements that form the nucleation sites of pseudotachylyte generation in previous models (John et al., 2009; Kelemen and Hirth, 2007). Future work to test this interpretation might involve high pressure fusion experiments, numerical modelling, detailed EBSD on more complex fault veins and geochemical analysis.

Acknowledgements

This work is supported Wits University, the National Research Foundation and the Mellon Foundation as well as the Research Council of Norway through its Centres of Excellence funding scheme, project number 223272 (CEED). Thanks to Prof. M. Zolensky of NASA for assisting with EBSD and XRD synchrotron analysis of some samples.

References

Agard, P., Monié, P., Jolivet, L., Goffé, B., 2002. Exhumation of the Schistes Lustrés complex: in situ laser probe $^{40}Ar/^{39}Ar$ constraints and implications for the Western Alps. J. Metamorph. Geol. 20, 599–618.

Andersen, T., Austrheim, H., 2006. Fossil earthquakes recorded by pseudotachylytes in mantle peridotite from the Alpine subduction complex of Corsica. Earth Planet. Sci. Lett. 242, 58–72.

Austrheim, H., Andersen, T.B., 2004. Pseudotachylytes from Corsica: fossil earthquakes from a subduction complex. Terra Nova 16, 193–197.

Austrheim, H., Boundy, T., 1994. Pseudotachylytes generated by seismic faulting and eclogitization of the deep crust. Science 265, 82–83.

Beccaluva, L., Ohnenstetter, D., Ohnenstetter, M., Venturelli, G., 1977. The trace element geochemistry of Corsican ophiolites. Contrib. Miner. Pet. 64, 11–31.

Bestmann, M., Pennacchioni, G., Frank, G., Göken, M., de Wall, H., 2011. Pseudotachylyte in muscovite-bearing quartzite: coseismic friction-induced melting and plastic deformation of quartz. J. Struct. Geol. 33, 169–186.

Braeck, S., Podladchikov, Y., 2007. Spontaneous thermal runaway as an ultimate failure mechanism of materials. Phys. Rev. Lett. 98.

Branlund, J.M., Kameyama, M.C., Yuen, D.A., Kaneda, Y., 2000. Effects of temperature-dependent thermal diffusivity on shear instability in a viscoelastic zone: implications for faster ductile faulting and earthquakes in the spinel stability field. Earth Planet. Sci. Lett. 182, 171–185.

Green, D.H., 1973. Experimental melting studies on a model upper mantle composition at high pressure under water-saturated and water-undersaturated conditions. Earth Planet. Sci. Lett. 19, 37–53.

Green, H.W., Houston, H., 1995. The mechanics of deep earthquakes. Annu. Rev. Earth Planet. Sci. 23, 169–213.

Hacker, B.R., 2003. Subduction factory 2. Are intermediate-depth earthquakes in subducting slabs linked to metamorphic dehydration reactions? J. Geophys. Res. 108.

Hobbs, B.E., Ord, A., Teyssier, C., 1986. Earthquakes in the ductile regime? Pure Appl. Geophys. J. R. Astron. Soc. 124, 309–336.

Jessell, M.W., Lister, G.S., 1991. Strain localization behaviour in experimental shear zones. Pure Appl. Geophys. 137, 421–438.

Jin, D., Karato, S., Obata, M., 1998. Mechanisms of shear localization in the continental lithosphere: inference from the deformation microstructures of peridotites from the Ivrea zone, northwestern Italy. J. Struct. Geol. 20, 195–209.

John, T., Medvedev, S., Rüpke, L.H., Andersen, T.B., Podladchikov, Y.Y., Austrheim, H., 2009. Generation of intermediate-depth earthquakes by self-localizing thermal runaway. Nat. Geosci. 2, 137–140.

John, T., Schenk, V., 2006. Interrelations between intermediate-depth earthquakes and fluid flow within subducting oceanic plates: constraints from eclogite facies pseudotachylytes. Geology 34, 557.

Jolivet, L., 1993. Extension of thickened continental crust, from brittle to ductile deformation: examples from Alpine Corsica and Aegean Sea. Ann. Geofis. 36, 139–153.

Jung, H., Green, H.W., Dobrzhinetskaya, L., 2004. Intermediate-depth earthquake faulting by dehydration embrittlement with negative volume change. Nature 428, 545–549.

Kameyama, M., Yuen, D.A., Karato, S.-I., 1999. Thermal–mechanical effects of low-temperature plasticity (the Peierls mechanism) on the deformation of a viscoelastic shear zone. Earth Planet. Sci. Lett. 168, 159–172.

Kanamori, H., Anderson, D., Heaton, T., 1998. Frictional melting during the rupture of the 1994 Bolivian earthquake. Science 279, 839–842.

Kelemen, P.B., Hirth, G., 2007. A periodic shear-heating mechanism for intermediate-depth earthquakes in the mantle. Nature 446, 787–790.

Kim, J.-W., Ree, J.-H., Han, R., Shimamoto, T., 2010. Experimental evidence for the simultaneous formation of pseudotachylyte and mylonite in the brittle regime. Geology 38, 1143–1146.

Kirby, S., Durham, W., Stern, L., 1991. Mantle phase changes and deep earthquake faulting in subducting lithosphere. Science 252, 216–225.

Lin, A., 1994. Glassy pseudotachylyte veins from Fuyun fault zone, northwest China. J. Struct. Geol. 16, 71–83.

Lund, M., Austrheim, H., 2003. High-pressure metamorphism and deep-crustal seismicity: evidence from contemporaneous formation of pseudotachylytes and eclogite facies coronas. Tectonophysics 372, 59–83.

Mancktelow, N.S., 2006. How ductile are ductile shear zones? Geology 34, 345.

Merlet, C., 1994. An accurate computer correction program for quantitative electron microprobe analysis. Mikrochim. Acta 114/115, 363–376.

Mohn, G., Manatschal, G., Muntener, O., Beltrando, M., Masini, E., 2009. Unravelling the interaction between tectonic and sedimentary processes during lithospheric thinning in the Alpine Tethys margins. Int. J. Earth Sci. 99, S75–S101.

Newman, J., Lamb, W., Drury, M.R., Vissers, R.L., 1999. Deformation processes in a peridotite shear zone: reaction-softening by an H_2O-deficient, continuous net transfer reaction. Tectonophysics 303, 193–222.

Ogawa, M., 1987. Shear instability in a viscoelastic material as the cause of deep focus earthquakes. J. Geophys. Res. 92, 13801–13810.

Ravna, E.J.K., Andersen, T.B., Jolivet, L., De Capitani, C., 2010. Cold subduction and the formation of lawsonite eclogite — constraints from prograde evolution of eclogitized pillow lava from Corsica. J. Metamorph. Geol. 28, 381–395.

Sibson, R.H., 1980. Transient discontinuities in ductile shear zones. J. Struct. Geol. 2, 165–171.

Silkoset, P., 2013. Microstructure of Ultramafic Pseudotachylyte From Alpine Corsica — Insights Into Earthquakes in Mantle Lithosphere. Unpublished Master thesis: University of Oslo, Norway.

Spray, J., 1992. A physical basis for the frictional melting of some rock-forming minerals. Tectonophysics 204, 201–221.

Vitale Brovarone, Groppo, Hetenyi, Compagnoni, R., Malavieille, 2011. Coexistence of lawsonite-bearing eclogite and blueschist: phase equilibria modelling of Alpine Corsica metabasalts and petrological evolution of subducting slabs. J. Metamorph. Geol. 29, 583–600.